

## Dual-Frequency Addressed Variable Optical Attenuator with Submillisecond Response Time

Xiao LIANG, Yan-Qing LU, Yung-Hsun WU, Fang DU, Hai-Ying WANG and Shin-Tson WU

College of Optics and Photonics, University of Central Florida, Orlando, Florida 32816, U.S.A.

(Received September 16, 2004; accepted December 2, 2004; published March 8, 2005)

We demonstrated a submillisecond response time and low-voltage variable optical attenuator (VOA) using a dual-frequency liquid crystal. The dynamic range of the VOA reaches 43 dB at a 1.55 μm wavelength. A normally on VOA with a flat wavelength response is obtained using a phase compensation cell. Fast rise and decay times are achieved using low-frequency overdrive and high-frequency undershoot voltages. Other approaches to further improve the VOA's performances are discussed. [DOI: 10.1143/JJAP.44.1292]

**KEYWORDS:** variable optical attenuator, liquid crystal devices, fast response time, dual-frequency addressing, overdrive and undershoot voltages

### 1. Introduction

Liquid crystal (LC)-based variable optical attenuators (VOAs) have been developed for fiber-optic communications at  $\lambda = 1.55 \mu\text{m}$  because of their low cost, low loss, and low power consumption.<sup>1–3)</sup> However, for most telecommunications applications, a fast response time and a large dynamic range (>30 dB) are required. Two types of LC-VOAs have been developed, nematic and ferroelectric.<sup>4)</sup> The latter is capable of achieving a microsecond response time, but it is a bistable device. To obtain gray scales, a pulse width modulation method has to be implemented. However, it is difficult to apply this technique to telecommunications products due to rigorous stability and reliability requirements. There are two major technical challenges for ferroelectric LCs: an ultra-thin cell gap ( $d < 2 \mu\text{m}$ ) and a residual DC voltage effect. The thin-cell requirement lowers the manufacturing yield and the residual DC voltage causes gray-scale instability. On the other hand, nematic VOA is easy to fabricate and it has natural gray scales. The major disadvantage is a slow response time. To achieve a fast response time, a small cell gap,<sup>5)</sup> a high-temperature effect,<sup>6,7)</sup> dual-frequency LC materials,<sup>8–10)</sup> a voltage effect,<sup>11,12)</sup> and a polymer-network LC<sup>13)</sup> were realized. A typical nematic LC-based VOA has a response time of approximately 5–15 ms, which is still slower than a mechanical shutter whose response time is approximately 1 ms. To outperform the mechanical shutter, the nematic VOA should have a submillisecond response time at room temperature while maintaining a wide dynamic range and low operating voltage ( $\leq 20 \text{ V}_{\text{rms}}$ ).

In this study, we demonstrated a fast-response and wide-dynamic-range nematic VOA using a high-birefringence and low-viscosity dual-frequency LC mixture. To achieve a submillisecond response time at room temperature ( $T \sim 21^\circ\text{C}$ ), we used a low-frequency ( $f = 1 \text{ kHz}$ ) overdrive voltage to decrease rise time and a high-frequency ( $f = 30 \text{ kHz}$ ) undershoot voltage to accelerate the decay process. The measured dynamic range exceeds 40 dB at  $\lambda = 1.55 \mu\text{m}$ .

### 2. Experimental Results

Figure 1 shows a schematic of the LC-based VOA, where two polarization beam displacers and an LC cell are sandwiched between two identical fiber collimators with

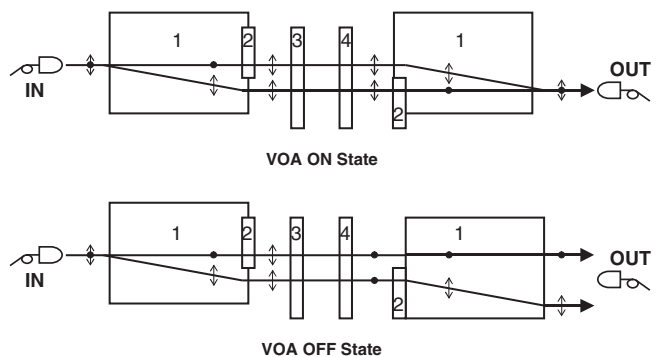


Fig. 1. Schematic diagram of DFLC-based variable optical attenuator, where "1", "2", "3" and "4" represent polarization beam displacer, half-wave plate, master LC cell, and compensation cell, respectively.

an 80 mm working distance. The light from the input fiber is collimated by the first GRIN (gradient index) lens collimator. When the light is incident to the first polarization beam displacer (PBD), a 10-mm-thick 45°-cut calcite crystal, it is separated into an ordinary beam and an extraordinary beam. A quartz half-wave plate (HWP) is laminated to the calcite PBD to rotate the polarization state of the top beam. Therefore, both beams have the same polarization before entering the LC cell. Here, we use a 3.7 μm homogeneous cell with its rubbing direction oriented at 45° to the input light polarization. Its phase retardation ( $\delta = 2\pi d \Delta n / \lambda$ ) is approximately  $1.2\pi$  at  $\lambda = 1.55 \mu\text{m}$ . To ensure a high transmittance at  $V = 0$ , an identical LC cell, i.e., with the same cell gap, LC material and alignment but with no voltage applied, was placed behind the master LC cell to act as a phase compensation cell. The rubbing direction of the compensation cell is orthogonal to that of the master cell so that the net phase retardation at  $V = 0$  is zero. This master compensation cell configuration exhibits an excellent wavelength tolerance.<sup>14)</sup> Under such circumstances, the top and bottom beams are recombined by the second PBD and HWP and then coupled into the collecting fiber collimator, as shown in the upper part of Fig. 1. This is the high-transmittance state of the VOA. To make the device compact, the compensation LC cell can be replaced with a polymeric film, which is used in display devices to increase the viewing angle.<sup>15)</sup>

When a proper voltage is applied to the master LC cell to make a  $\pi$  phase change, the incident beams could not retain their original polarizations. As a result, they are separated by the second beam displacer. No light is coupled into the collecting fiber collimator and the off-state results, as shown in Fig. 1. By tuning the master cell voltage, different gray scales can be obtained. If the LC cell gaps are all uniform, then the VOA should have no polarization-dependent loss (PDL) and no polarization mode dispersion (PMD). In our experiments, the beam displacers and the LC cell are tilted at a small angle to avoid back reflections (not illustrated in the diagram).

The VOA performance is mainly determined by the LC material employed. To achieve a fast response time, we decided to use a dual-frequency liquid crystal (DFLC). The key feature of a DFLC is that it exhibits a cross-over frequency ( $f_c$ ). In the  $f < f_c$  region, the dielectric anisotropy ( $\Delta\epsilon$ ) is positive, while in the  $f > f_c$  region the  $\Delta\epsilon$  becomes negative. In the low-frequency region, the electric-field-induced torque reorients the LC molecules along the field direction. This leads to the fast rise time. During the relaxation period, a high-frequency electric field is applied to the cell. Because the  $\Delta\epsilon$  is negative, the high-frequency electric field helps to accelerate the relaxation of the LC molecules to their original positions. As a result, a fast decay time is achieved.

Most of the commercially available DFLC mixtures have a low birefringence, high viscosity, and small  $|\Delta\epsilon|$  values.<sup>9</sup> Due to their low birefringence, a thick LC layer is required, particularly for the  $1.55 \mu\text{m}$  infrared wavelength. The thick LC layer leads to a slow response time and a high operating voltage. To overcome these drawbacks, we prepared a high-birefringence and low-viscosity DFLC mixture using 30% biphenyl esters and 70% lateral difluoro tolanes. The physical properties of our DFLC mixture at room temperature ( $T = 21^\circ\text{C}$ ) are summarized as follows: cross-over frequency  $f_c \approx 4 \text{ kHz}$ ;  $\Delta n = n_e - n_o = 0.25$  at  $\lambda = 1.55 \mu\text{m}$ ;  $\Delta\epsilon = 4.73$  at  $f = 1 \text{ kHz}$ ; and  $\Delta\epsilon = -3.93$  at  $f = 30 \text{ kHz}$ .

For VOA demonstration, we used an Ando AQ4321D tunable laser operated at  $\lambda = 1.55 \mu\text{m}$  as the light source. The output fiber was connected to an Ando AQ8201-21 power monitor for measuring transmittance. A computer-controlled LabVIEW system was used for data recording and processing. The insertion loss (IL) of our VOA at  $V = 0$  was measured to be approximately  $-2.0 \text{ dB}$  (without connector). The PDL remains less than  $0.1 \text{ dB}$  over the whole ITU (International Telecommunication Union) C-band ( $1.53\text{--}1.57 \mu\text{m}$ ) as expected. Although the measured IL is still not sufficiently low, the actual fiber-to-fiber coupling loss is only approximately  $0.8 \text{ dB}$  when taking into account the  $\sim 1.2 \text{ dB}$  propagation loss which is mainly contributed by the uncoated LC cells.

Figure 2 shows the VOA attenuation measured at different driving voltages. The VOA is addressed by square waves at  $f = 1 \text{ kHz}$ . Because of the positive  $\Delta\epsilon$  in the low-frequency region, the LC molecules are reoriented along the electric-field direction as the voltage exceeds  $2.5 \text{ V}_{\text{rms}}$  (threshold voltage). At  $V = 6 \text{ V}_{\text{rms}}$  which corresponds to a  $\pi$  phase change, an off state with  $-43 \text{ dB}$  attenuation is achieved. As shown in Fig. 2, this off state is quite stable.

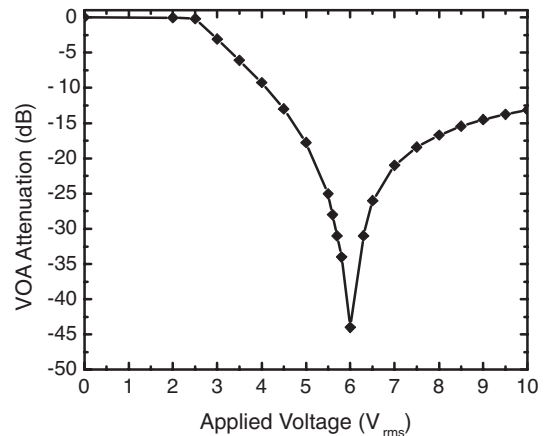


Fig. 2. Measured VOA attenuation on dB scale as function of applied voltage. The VOA is addressed by a  $1 \text{ kHz}$  square-wave ac source.

Within  $\pm 0.3 \text{ V}_{\text{rms}}$  voltage variation, the measured attenuation remains of over  $-30 \text{ dB}$ , which is important if this VOA is to be used as a light switch or wavelength blocker. As the applied voltage exceeds  $6 \text{ V}_{\text{rms}}$ , the net phase change due to the orthogonal master and compensation cells is deviated from  $1\pi$  so that the optimal off state condition is no longer satisfied. As a result, the VOA attenuation gradually decreases.

To improve the VOA response time, we applied the overdrive and undershoot voltage waveforms during the low- and high-frequency periods, respectively, to drive the master cell while keeping the compensation cell uncharged. The low-frequency voltage was used to reorient the LC molecules and the high-frequency voltage was used to erase this reorientation. Results are compared with those using the conventional single-frequency driving method as shown in Fig. 3. The solid lines in Figs. 3(a) and 3(b) show the turn-off and turn-on times, when a  $6 \text{ V}_{\text{rms}}$  single-frequency ( $f = 1 \text{ kHz}$ ) voltage is applied and removed from the cell, respectively. The 90–10% and 10–90% transmittance transition times are  $11 \text{ ms}$  and  $35 \text{ ms}$ , respectively. From Fig. 3(a), the unbiased case has a delay time of  $\sim 4 \text{ ms}$ . To reduce the delay time, we applied a  $1 \text{ kHz}$ ,  $2 \text{ V}_{\text{rms}}$  biased voltage, which is somewhat lower than the threshold voltage ( $V_{\text{th}} \sim 2.5 \text{ V}_{\text{rms}}$ ). The turn-off time, the dashed line in Fig. 3(a), is indeed reduced. However, the relaxation time (dashed lines) as depicted in Fig. 3(b) was increased to  $\sim 60 \text{ ms}$ .

Figure 4 shows the turn-on and turn-off times of the DFLC cell with the overdrive and undershoot voltages applied during the rise and decay periods. The commercial LC-VOA is normally driven by a  $20 \text{ V}$  ac voltage source. For a fair comparison, we also limited our overdriving voltage to  $20 \text{ V}_{\text{rms}}$ . The  $20 \text{ V}_{\text{rms}}$  low-frequency voltage burst was applied for  $2 \text{ ms}$  between the  $2 \text{ V}_{\text{rms}}$  bias and  $6 \text{ V}_{\text{rms}}$  holding voltages. The turn-on time (90–10%) was measured to be  $0.73 \text{ ms}$ . The overdrive voltage signals and the corresponding optical responses are illustrated in Fig. 4(a).

During the relaxation process, the constant bias voltage exerts a torque to resist LC molecules returning to their original positions. To overcome this bottleneck, a high-frequency ( $f = 30 \text{ kHz}$ ) voltage was imposed before apply-

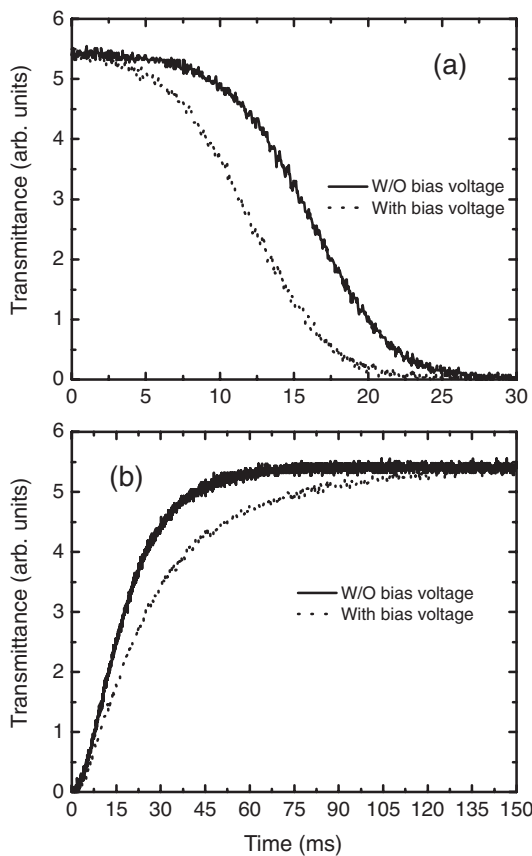


Fig. 3. (a) Optical response curves of DFLC VOA when 1 kHz 6 V<sub>rms</sub> voltage is applied to turn VOA to off state. (b) Optical response curves that reflect LC directors' relaxation process when applied field is removed. The solid line and dot line correspond to cases without and with a 2 V<sub>rms</sub>-bias voltage ( $f = 1$  kHz), respectively.

ing the bias voltage. The LC decay was thus accelerated, as depicted in Fig. 4(b). This is known as the undershoot effect. The decay time (10–90%) was suppressed to 0.78 ms, which is approximately an order of magnitude faster than that of a commercial LC-VOA. From Fig. 4(b), the 2 ms undershooting pulses are slightly longer than the required duration, which means that the decay process may even be somewhat improved for an optimized undershooting burst.

### 3. Discussions

The response times studied above are all between the VOA's "on" and "off" states. However, the dual frequency overdriving and undershooting also apply to the fast grayscale transition between two arbitrary attenuation states. A high-voltage (*e.g.*, 20 V<sub>rms</sub>) burst of suitable frequency and duration may be inserted between the initial and target states to accelerate the LC director's rise or decay.

To further improve the VOA's response time, a DFLC with a higher dielectric anisotropy and a lower rotational viscosity is preferred. For some specific applications, we could increase the overdrive and undershoot voltages to further reduce response time. However, for normal fiber-optic applications, a high voltage is rarely used. Another simple and effective alternative is to use a reflective-type VOA, where the incident light passes the LC layer twice so that a cell with a half thickness may provide the same phase retardation. Because the free-relaxation response time  $\tau_0$  is

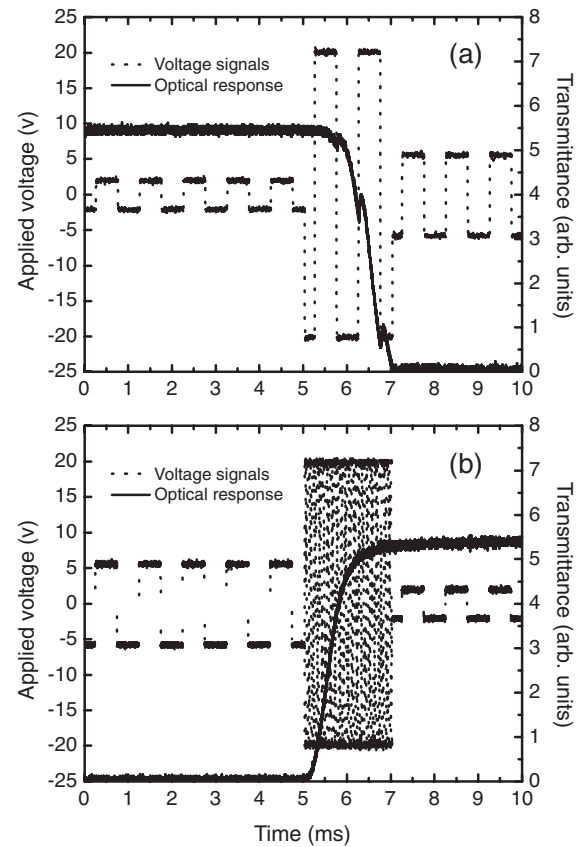


Fig. 4. Overdrive and undershoot voltages and corresponding optical responses.

proportional to the square of the cell gap, a four-times-faster response may be achieved. The only performance sacrifice is the slightly increased insertion loss due to the double pass. Although our demonstrated VOA is a normally on device, it can also work in the normally off mode if the phase compensation cell changes  $\pi$  (*or*  $\pi/2$ ) phase retardation, where  $\pi$  (*and*  $\pi/2$ ) corresponds to that of transmissive-type (*and* reflective-type) VOAs.

### 4. Conclusions

In summary, we proposed a DFLC-based infrared VOA with a 43 dB dynamic attenuation range at room temperature. The submillisecond rise and decay times were achieved by integrating a 3.7  $\mu\text{m}$  small cell gap and high-performance dual-frequency LC material, as well as the overdrive and undershoot voltage technique.

This work is supported by AFOSR under contract No. F49620-01-1-0377.

- 1) C. Mao, M. Xu, W. Feng, T. Huang, K. Wu and J. Wu: Proc. SPIE **5003** (2003) 121.
- 2) L. Eldada: Rev. Scientific Instrum. **75** (2004) 575.
- 3) J. J. Pan, H. Wu, W. Wang, X. Qiu and J. Jiang: Proc. National Fiber Optics Engineers Conference, Telcordia, Orlando, 2003, p. 943.
- 4) N. A. Riza and S. F. Yuan: J. Lightwave Technol. **17** (1999) 1575.
- 5) S. T. Wu and U. Efron: Appl. Phys. Lett. **48** (1986) 624.
- 6) V. V. Belyaev, S. Ivanov and M. F. Grebenkin: Sov. Phys. Crystallogr. **30** (1985) 674.
- 7) S. T. Wu, U. Efron and A. M. Lackner: Appl. Opt. **26** (1987) 3411.
- 8) H. K. Bucher, R. T. Klingbiel and J. P. VanMeter: Appl. Phys. Lett. **25**

- (1974) 186.
- 9) M. Schadt: Mol. Cryst. Liq. Cryst. **89** (1982) 77.
  - 10) M. Xu and D. K. Yang: Appl. Phys. Lett. **70** (1997) 720.
  - 11) I. C. Khoo and S. T. Wu: *Optics and Nonlinear Optics of Liquid Crystals* (World Scientific, Singapore, 1993).
  - 12) S. T. Wu: Appl. Phys. Lett. **57** (1990) 986.
  - 13) Y. Q. Lu, F. Du, Y. H. Lin and S. T. Wu: Opt. Express **12** (2004) 1221.
  - 14) S. T. Wu: J. Appl. Phys. **73** (1993) 2080.
  - 15) S. T. Wu and D. K. Yang: *Reflective Liquid Crystal Displays* (Wiley, New York, 2001).